


Space Debris Laser Ranging with range-gate-free Superconducting Nanowire Single-Photon Detector

Haitao Zhang¹ , Yuqiang Li^{1,2,*}, Zhulian Li^{1,2}, Xiaoyu Pi¹, Yongzhang Yang¹, and Rufeng Tang¹

¹ Group of Applied Astronomy, Yunnan Observatories, Chinese Academy of Sciences, Kunming 650216, China

² Key Laboratory of Space Object & Debris Observation, PMO, CAS, Nanjing 210008, China

Received 3 November 2022 / Accepted 10 January 2023

Abstract. Space Debris Laser Ranging (DLR) is a technique to measure range to defunct satellites, rocket bodies or other space targets in orbits around Earth. The analysis shows that one of the reasons for the low success probability of DLR is the inaccurate orbital prediction of targets. Then it is proposed to use the Superconducting Nanowire Single-Photon Detector (SNSPD) running in automatic-recoverable range-gate-free mode, in which case, the effect of the accuracy of the target's orbital prediction on the success probability of DLR is greatly reduced. In this way, 249 space debris were successfully detected and 532 passes of data were obtained. The smallest target detected was the space-debris (902) with an orbital altitude of about 1000 km and a Radar Cross Section (RCS) of 0.0446 m². The farthest target detected was the space-debris (12,445) with a large elliptical orbit and an RCS of 18.2505 m², of which the range of the normal point (NPT) of the measured arc-segment on January 27, 2019 was 6260.805 km.

Keywords: Space Debris Laser Ranging, The success probability of DLR, Range-gate-free mode, Superconducting Nanowire Single-Photon Detector.

1 Introduction

Satellite Laser Ranging (SLR) is a technique to measure range to cooperative targets (targets with retro-reflectors). Laser ranging activities are organized under the International Laser Ranging Service (ILRS), which provides global SLR data and its derived data to support research in geodesy, geophysics, and fundamental constants. Because of its high accuracy, SLR has been highly valued and developed in the field of space targets measurement and monitoring [1, 2].

Space Debris Laser Ranging (DLR) technology is developed from SLR technology, and DLR is a technique to measure range to non-cooperative targets (targets without retro-reflectors). Comparing with SLR, DLR is more difficult, which mainly results from the low reflectivity of targets and the inaccurate orbital prediction of targets [3–8].

In recent years, the development of DLR technology has focused on improving the echo detection capability of DLR systems, such as higher laser single-pulse energy [8], near-infrared wavelength ranging [9], multi-pulse ranging [10, 11], single-station transmitting and multi-station receiving [12–14], high-sensitivity detectors [15, 16], and many other techniques.

However, the success probability of DLR is determined by both detection probability and false alarm probability. In order to suppress noise and keep the false alarm probability at a low level, the range gate is commonly used, which relies on high-accuracy prediction to calculate the exact opening time of the range gate. The representative Two Line Element (TLE) within 24-h provides orbital prediction of space debris with an accuracy of hundreds of meters or even kilometers, while the ILRS provides the Consolidated Prediction Format (CPF) for cooperative targets with an accuracy of meters.

In terms of improving the accuracy of orbital prediction of space debris, the accuracy of a limited number of targets can be improved by using the generated short-arc-length DLR data or fused optical angle measurement data, but it is based on a prerequisite that we could obtain DLR data, which cannot meet the high real-time requirements of DLR for high-accuracy prediction [17, 18]. The Range Bias (RB) of orbital prediction can be indirectly reduced to a certain extent by calculating and applying the Time Bias (TB) of the along-track [19], and the Austrian Graz SLR station applies the real-time TB to reduce the search range in daylight space debris laser ranging [3, 20], but it still cannot directly correct the RB in the radial direction.

By analyzing the success probability of DLR, it is proposed to use a new detector running in automatic-recoverable

* Corresponding author: lyq@ynao.ac.cn

range-gate-free mode, which can greatly reduce the effect of the inaccurate orbital prediction of targets. Superconducting Nanowire Single-Photon Detector (SNSPD) is a novel detector for efficient, fast, and accurate detection of single photons with the advantages of low dark count rate, high detection rate, and wide detection spectrum, which has potential applications in many fields [16, 21–23]. And the SNSPD can automatically recover its working state in range-gate-free mode. This method increases the probability of detection and reduces the false alarm probability of DLR, thus increasing the success probability of DLR.

2 DLR in normal mode and range-gate-free mode

In SLR, the range gate can effectively prevent the interference from noise, in which the accurate orbital prediction of targets is required to calculate the opening time of the range gate. The orbital prediction of the cooperative targets is so accurate that the range gate is opened only a split second before the arrival of the expected echo photons, then the detector starts to work, thus reducing the interference of the noise photons [24, 25].

The probability of detecting an echo photon at the time of its arrival (detection probability) is expressed as equation (1) [24, 25]:

$$p_s = (1 - e^{-(n_s+n_n\tau)}) \left(\frac{n_s}{n_s + n_n\tau} \right), \quad (1)$$

where n_s is the number of echo photons reaching the detector, n_n is the noise-photon rate reaching the detector, and τ is the response time of the detector. The probability of the detector being triggered by noise photons during the period when the detector is waiting for the echo photons after the range gate is opened (false alarm probability) is expressed as equation (2) [24, 25]:

$$p_n = 1 - e^{-n_n t_{rg}}, \quad (2)$$

where t_{rg} is the period when the detector is waiting for the echo photons after the range gate is opened, which is the advance of the opening time of the range gate. The success probability of laser ranging depends on the echo photon detection probability and the false alarm probability, expressed as equation (3) [24, 25]:

$$p = (1 - p_n)p_s. \quad (3)$$

The detection principle of DLR is the same as SLR. The detector with a range gate (in normal mode) can respond once for each laser pulse. As shown in Figure 1, at the m th pulse, the timing advance and the orbit-prediction bias are included in the period from the opening time of the range gate to the echo arrival time. It is possible to detect an echo photon only if the detector is not triggered by noise photons during this period. The orbit-prediction bias is always changing during DLR, at the n th pulse, the range gate opens after the arrival of the echo due to

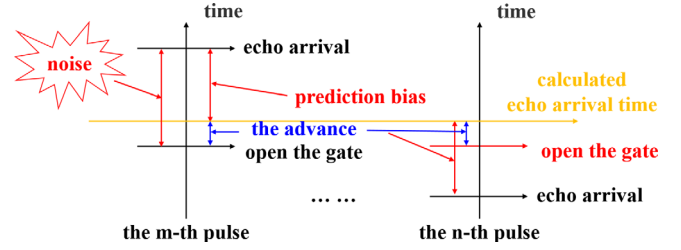


Fig. 1. The process of each pulse for DLR in normal mode.

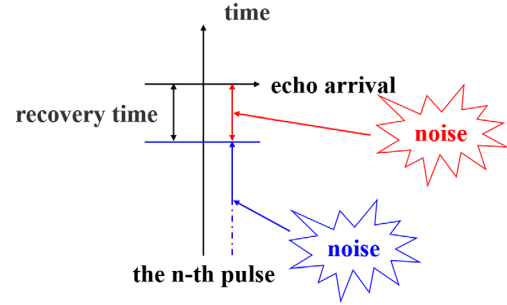


Fig. 2. The process of each pulse for DLR in range-gate-free mode.

the orbit-prediction bias, and it is impossible to detect an echo photon. The false alarm probability is expressed as equation (4):

$$p_n = 1 - e^{-n_n(t_{pb}+t_{rg})}, \quad (4)$$

where t_{pb} is the orbit-prediction bias.

The SNSPD can automatically recover its working state in range-gate-free mode [26, 27], and for each laser pulse, the SNSPD can respond multiple times. As shown in Figure 2, it is possible for the SNSPD to detect an echo photon as long as the detector is not triggered by noise photons during a recovery time before the echo photons' arrival, and the false alarm probability of DLR with a range-gate-free SNSPD is expressed as equation (5):

$$p_n = 1 - e^{-n_n t_{rt}}, \quad (5)$$

where t_{rt} is the recovery time.

The DLR data in normal mode are shown in Figure 3a. It can be seen from the figure that most of the data were obtained within a short period after the range gate is opened, which indicates that the photons arriving at the detector at the instant of the range gate is opened are more likely to be detected. And the opening time of the range gate is calculated based on the orbital prediction of the target. As shown in Figure 3a, the opening time of the range gate need to be searched continuously during DLR, because the accuracy of orbital prediction of target is poor and the orbit-prediction bias is always changing.

The DLR data in range-gate-free mode is shown in Figure 3b. As long as the echo photons are within the threshold of Observed-minus-Calculated (O-C), the success probability of laser ranging in range-gate-free mode is not affected by the accuracy of the target's orbital prediction. And we no longer need to continuously search the opening

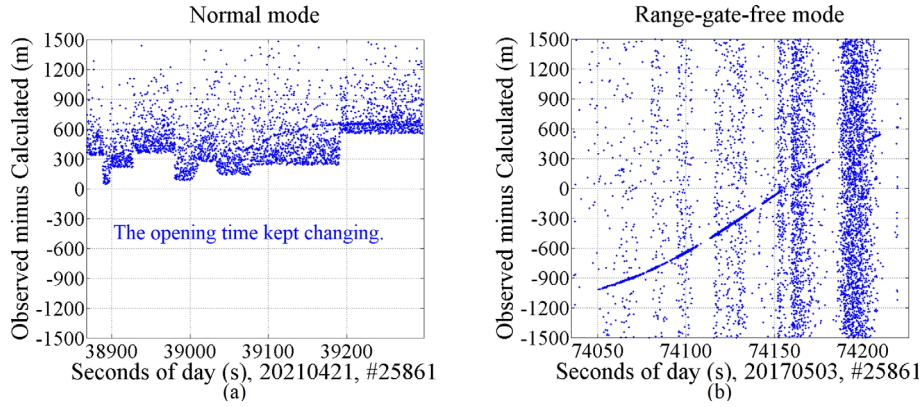


Fig. 3. The DLR data in normal mode and range-gate-free mode. (a) The DLR data in normal mode. (b) The DLR data in range-gate-free mode.

time of the range gate during DLR, while the search process relies on experience and luck.

According to equations (1) and (3)–(5), the success probability of DLR is calculated (the slant range between station and the target is 1000 km, the optical cross section of the target is 1 m²), and the results are shown in Figure 4. Under the same conditions, DLR in range-gate-free mode is more likely to detect the target than DLR in normal mode when the accuracy of the target’s orbital prediction is poor.

We used an inaccurate orbital prediction in the experiment, and some data are shown in Figure 5. As shown in Figure 5a, the Time Bias (TB) of the orbital prediction is 246 milliseconds and the Range Bias (RB) of the orbital prediction is −493.4 m. As shown in Figure 5b, the TB of the orbital prediction is −108.38 milliseconds and the RB of the orbital prediction is 1355.5 m. In range-gate-free mode, the targets were successfully detected with a poor accuracy of orbital prediction.

In this way, it is possible to obtain the echo data even when the target is invisible, the data is shown in Figure 6. The target was invisible at that time, we tried to keep searching for the pointing of telescope to aim at the target and finally detected the echo. And the vertical lines in the O-C chart of Figures 3, 5 and 6 may result from the response of the detector to strong noise, such as backscatter.

3 Experiment and results

As shown in Figure 7 [28], the system uses a 53 cm binocular to transmit laser pulses to the space debris and a 1.2 m telescope to receive echo photons reflected by the target [23, 28]. Usually, the range gate is used to reduce the background noise as a time-filter technique, in range-gate-free mode, the method of transmitting from one telescope and receiving from another is designed to reduce the effect of backscatter noise. In order to further improve the success probability of DLR, we use a range-gate-free SNSPD array and transform multiple GT668 time interval analyzers into a multi-channel event timer through software development. The elements of the SNSPD array respond to photons independently and output signals to the multi-channel event timer. The system parameters are shown in Table 1.

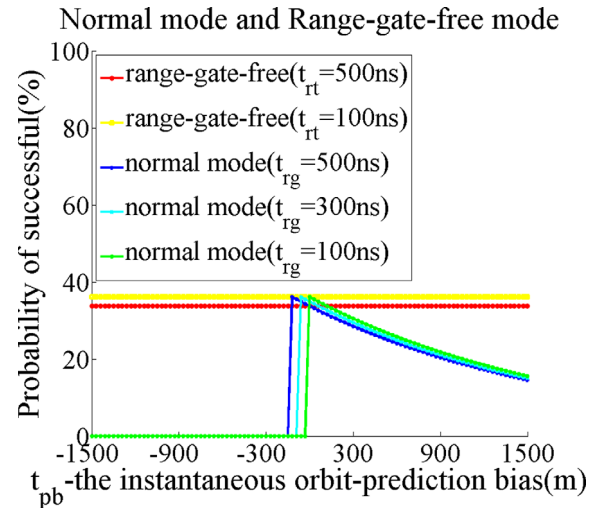


Fig. 4. Comparison of normal mode and range-gate-free mode.

Assuming that the number of pixels of the SNSPD array is w , the detection efficiency of each pixel is equal ($\eta_1 = \eta_2 = \dots = \eta_w = \eta_{\text{pixel}}$), and each pixel is independent of each other, the success probability of laser ranging for each pixel is p_{pixel} , the success probability of laser ranging with a range-gate-free SNSPD array is expressed as equation (6):

$$p_{\text{array}} = 1 - (1 - p_{\text{pixel}})^w = 1 - \left(1 - e^{-n_n t_{\text{rt}}} (1 - e^{-(n_s + n_n \tau)}) \left(\frac{n_s}{n_s + n_n \tau}\right)\right)^w. \quad (6)$$

The number of echo photons is calculated according to the laser ranging equation (7) [29]:

$$n_s = \frac{E_t}{h\nu} \eta_t \frac{2}{\pi(\theta_d R)^2} e^{-\left(\frac{\Delta\theta_p}{\theta_d}\right)^2} \left(\frac{1}{1 + \left(\frac{\Delta\theta_s}{\theta_d}\right)^2}\right) \times \left(\frac{\rho\sigma A_r}{4\pi R^2}\right) \eta_r \eta_c T_a^2 T_c^2, \quad (7)$$

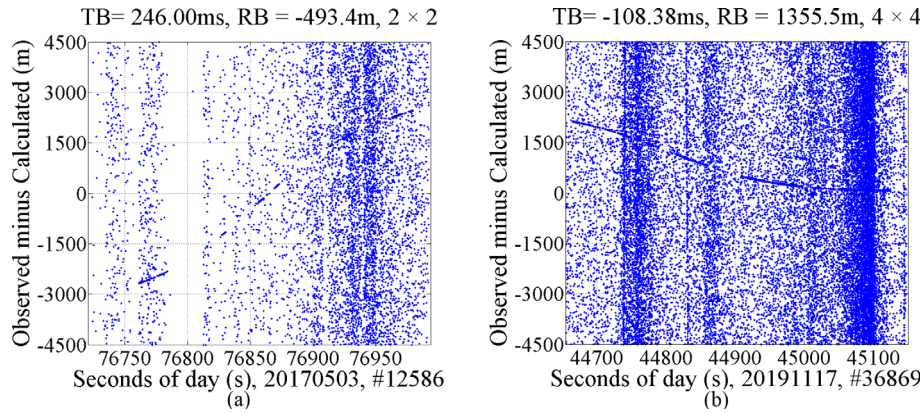


Fig. 5. The DLR data, the TB and RB of the orbital prediction are relatively large. (a) The TB of the orbital prediction is 246 ms. (b) The RB of the orbital prediction is 1355.5 m.

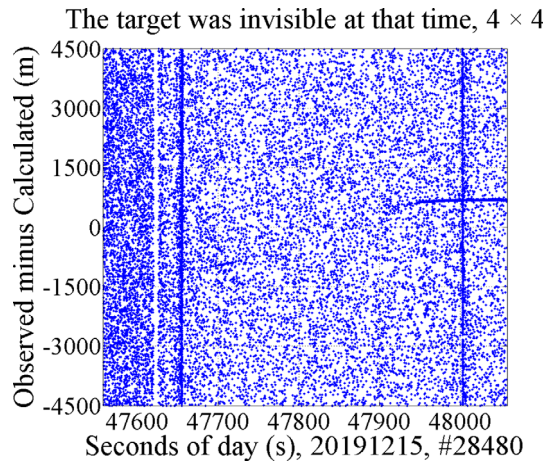


Fig. 6. The DLR data, the target was invisible at that time.

where the laser ranging system parameters are shown in Table 1, R is the slant range between station and space-debris, ρ is the reflectivity of space-debris, and σ is the optical cross section of space-debris.

The noise-photon rate is mainly related to the noise-photon rate caused by the sky light background (n_b), the noise-photon rate caused by the target brightness (n_t), and the detector dark count rate (n_{dcr}), which can be expressed as equation (8) [30]:

$$n_n = n_b + n_t + n_{dcr} + \dots, \quad (8)$$

n_b and n_t are calculated according to the empirical equation (9) [24, 25]:

$$n_b + n_t = \frac{\pi}{4} (N_n + N_t) \theta_r^2 A_r q \eta_r \eta_c. \quad (9)$$

The 2×2 and 4×4 of SNSPD arrays were used in the DLR system, and the probabilities of success for DLR of different sizes and ranges of space-debris has been calculated, the results are shown in Figure 8, in which the laser single-pulse energy is 400 mJ.

In 2017–2019, an 87-day observation experiment was conducted. During the experiment, 249 space debris were detected and 532 passes of data were obtained. And the session Root Mean Square (RMS, the session RMS from the mean of raw accepted time-of-flight values minus the trend function) of the Normal Point (NPT) data are less than 2 m.

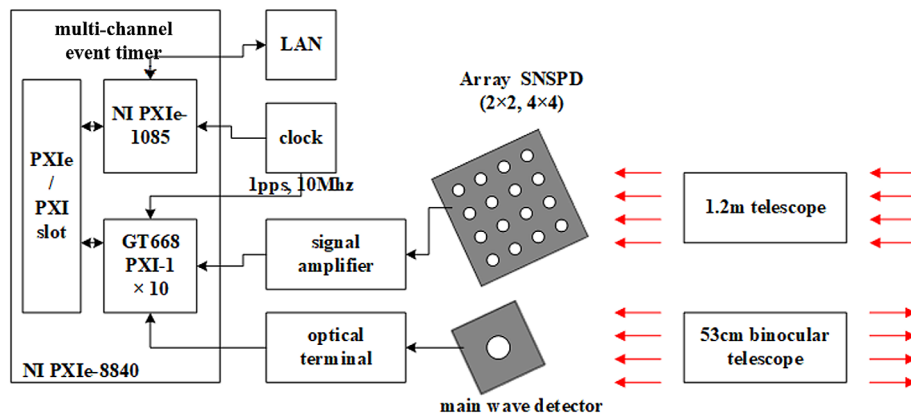


Fig. 7. Diagram of the DLR system.

Table 1. Parameters and values of the system.

Notation	Values	Parameters
Et	400–3000 mJ	Laser single-pulse energy, generally using 400 mJ
f_t	100 Hz	Laser repetition rate, laser power is 40–300 W
w_p	6.7 ns	Laser pulse width
$h\nu$	hc/λ , $\lambda = 1064$ nm	Photon energy, λ is laser wavelength
η_t	0.60	Transmitting optical system efficiency
θ_d	3''	Gaussian beam divergence half angle
θ_p	2''	Laser beam pointing error
θ_j	2''	RMS (Root Mean Square) tracking mount jitter
A_r	$\pi(d/2)^2$, $d = 1.2$ m	Telescope receive area
η_r	0.40	Receiving optical system efficiency
η_c	~32% @ 2×2 , ~80% @ 4×4	Detection efficiency, ~10% @ each pixel
τ	~200 ps	Detector response time
t_{rt}	~500 ns	Recovery time
n_{der}	<1 kHz/pixel	Dark count rate
T_a	0.60	One way atmospheric transmission
T_c	1.00	One way cirrus cloud transmission
θ_r	10''	Receiving view angle
q	10 nm	Bandwidth of filter
N_n	$\sim 3.4 \times 10^{19}$	Sky brightness of moonless night, unit: cps/($m^2 \times$ steradian)
N_t	$\sim 10^{23}$	Target brightness, unit: cps/($m^2 \times$ steradian)

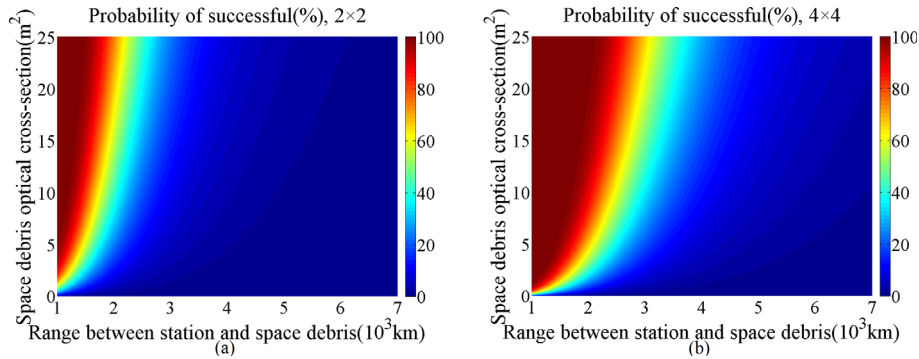


Fig. 8. The success probability of DLR with different sizes and ranges. (a) 2×2 SNSPD array and (b) 4×4 SNSPD array.

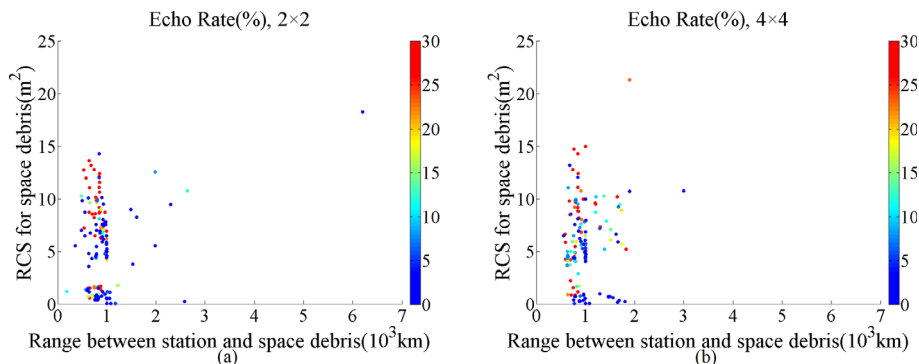


Fig. 9. The echo rate statistics for different targets. (a) 2×2 SNSPD array and (b) 4×4 SNSPD array.

The echo rate statistics for different targets are shown in Figure 9. The trend of echo rate for different targets is generally consistent with Figure 8, and the higher echo rates for some smaller sized targets are due to the higher laser single-pulse energy utilized during DLR. The smallest target detected in the experiment was the space-debris (902) with an orbital altitude of about 1000 km and a Radar Cross Section (RCS) of 0.0446 m^2 [28]. And the farthest target detected was the space-debris (12,445) with a large elliptical orbit and an RCS of 18.2505 m^2 , of which the range of the NPT of the measured arc-segment on January 27, 2019 was 6260.805 km.

4 Conclusion

The poor accuracy of orbital prediction of space debris is a challenge for space debris laser ranging. After achieving space debris laser ranging in 2010 [8], the Yunnan Observatories continued to conduct related research. And it is proposed to use the SNSPD array running in automatic-recoverable range-gate-free mode, which can greatly reduce the effect of the inaccurate orbital prediction of targets. The results show that the method increases the probability of detection and reduces the false alarm probability, thus increasing the success probability of space debris laser ranging. In the future, we will devote to applying the method to daylight space debris laser ranging and space debris laser ranging without orbital prediction.

Conflict of interest

The authors declare no conflicts of interest.

Funding

National Natural Science Foundation of China (NSFC) (11703086), Youth Innovation Promotion Association, CAS (Y201817), Yunnan Innovation Team (202105AE160017).

Data availability

Data underlying the results presented in this paper are not publicly available at this time but may be obtained from the authors upon reasonable request.

Acknowledgments. We are very grateful to engineer Dehua Ju, and observation assistant Chao He for their hard work in the observation experiment, and we appreciate Ms. Yanyun She for her help in polishing articles.

References

- 1 Degnan J.J. (1993) *Contributions of space geodesy to geodynamics: technology*, American Geophysical Union. pp. 133–162.
- 2 Kucharski D., Kirchner G., Koidl F., Fan C., Carman R., Moore C., Dmytrotso A., Ploner M., Bianco G., Medvedskij M. (2014) Attitude and spin period of space debris Envisat measured by satellite laser ranging, *IEEE Trans. Geosci. Remote Sens.* **52**, 7651.
- 3 Steindorfer M.A., Kirchner G., Koidl F., Wang Peiyuan, Jilete B., Flohrer T. (2020) Daylight space debris laser ranging, *Nat Commun.* **11**, 1, 3735.
- 4 Zhulian L., Haitao Z., Yuqiang L., Honglin F., Dongsheng Z. (2017) 53 cm binocular telescope high repetition frequency space debris laser ranging system, *Infrared Laser Eng.* **46**, 7, 0729001.
- 5 Xue D., Xingwei H., Qingli S., Zhipeng L., Cunbo F., Haitao Z. (2016) Research of space debris laser ranging system, *Infrared Laser Eng.* **45**, S2, S229002.
- 6 Zhang H., Deng H., Wu Z., Tang K., Zhang Z. (2016) Observations of space debris by ground-based laser ranging system, *Spacecraft Environ. Eng.* **33**, 5, 457–462.
- 7 Li Y., Li R., Li Z., Zhai D., Fu D., Xiong Y. (2015) Application research on space debris laser ranging, *Infrared Laser Eng.* **44**, 11, 3324–3329.
- 8 Li Y., Li Z., Fu H., Zheng X., He S., Zhai D., Xiong Y. (2011) Experimentation of diffuse reflection laser ranging of space debris, *Chin. J. Lasers* **38**, 0908001.
- 9 Meng W., Zhang H., Deng H., et al. (2020) 1.06 μm wavelength based high accuracy satellite laser ranging and space debris detection, *Acta Phys. Sin.* **69**, 1, 019502.
- 10 Zhang Z., Zhang H., Long M., Deng H., Wu Z., Meng W. (2019) High precision space debris laser ranging with 4.2 W double-pulse picosecond laser at 1 kHz in 532 nm, *Optik* **179**, 691–699.
- 11 Long M.L., Deng H.R., Zhang H.F. (2021) Development of multiple pulse picosecond laser with 1 kHz repetition rate and its application in space debris laser ranging, *Acta Opt. Sin.* **41**, 6, 0614001.
- 12 Kirchner G., Koidl F., Ploner M., Lauber P., Utzinger J., Schreiber U., Eckl J., Wilkinson M., Sherwood R., Giessen A., Weigel M. (2013) Multistatic laser ranging to space debris, in: *18th International Workshop on Laser Ranging*, Fujiyoshida, Japan, pp. 13–0213.
- 13 Zhang Z., Zhang H., Deng H., et al. (2016) Experiment of laser ranging to space debris by using two receiving telescopes, *Infrared Laser Eng.* **45**, 7, 0102002.
- 14 Li C., Li Z., Tang R., et al. (2020) Target distance measurement experiment with a bi-static satellite laser ranging system, *Infrared Laser Eng.* **49**, S1, 0200145.
- 15 Li Z., Zhai D., Zhang H., et al. (2020) Superconductivity detector applied to daytime satellite laser ranging experiment and research, *Infrared Laser Eng.* **49**, 8, 20190536.
- 16 Xue L., Li Z., Zhang L., Zhai D., Li Y., Zhang S., Li M., Kang L., Chen J., Wu P., Xiong Y. (2016) Satellite laser ranging using superconducting nanowire single-photon detectors at 1064 nm wavelength, *Opt. Lett.* **41**, 16, 3848–3851.
- 17 Sang J., Bennett J.C. (2014) Achievable debris orbit prediction accuracy using laser ranging data from a single station, *Adv. Space Res.* **54**, 1, 119–124.
- 18 Kim S., Lim H.C., Bennett J.C., et al. (2014) Analysis of space debris orbit prediction using angle and laser ranging data from two tracking sites under limited observation environment, *Sensors* **20**, 7, 1950.
- 19 Zhang X., Zhao X., Li R., et al. (2019) Research on real-time correction method of laser ranging prediction of non-cooperative target, *Astron. Res. Technol.* **16**, 1, 25–32.

- 20 Gao J., Liang Z., Han X., et al. (2022) Range prediction deviation real-time correction algorithm for space debris laser ranging, *Acta Photonica Sin.* **51**, 9, 0912002.
- 21 Lv C.L., Zhou H., Li H., You L.X., Liu X.Y., Wang Y., Zhang W.J., Chen S.J., Wang Z., Xie X.M. (2017) Large active area superconducting single-nanowire photon detector with a 100 μm diameter, *Supercond. Sci. Technol.* **30**.
- 22 LiXing Y. (2014) Recent progress on superconducting nanowire single photon detector, *Sci. Sin. Inform.* **44**, 3, 370–388.
- 23 Tang R., Li Z., Li Y., Pi X., Su X., Li R., Zhang H., Zhai D., Fu H. (2018) Light curve measurements with a superconducting nanowire single-photon detector, *Opt. Lett.* **43**, 21, 5488–5491.
- 24 Ye S., Huang C. (2000) *Astrogeodynamics*, Shandong Science & Technology Press. pp. 91–121.
- 25 Zhao C., Shang J., Feng Q., Guo J., Wei Z., Li Y. (2016) *Space object laser ranging technology and its applications*, Science Press. pp. 44–56.
- 26 Chen Q., Zhang B., Zhang L. (2020) Sixteen-pixel NbN nanowire single photon detector coupled with 300- μm fiber, *IEEE Photonics J.* **12**, 1, 1–12.
- 27 Zhang L., Wan C., Gu M., Xu R., Zhang S., Kang L., Chen J., Wu P. (2015) Dual-lens beam compression for optical coupling in superconducting nanowire single-photon detectors, *Sci. Bull.* **60**, 1434–1438.
- 28 Haitao Z., Zhulian L., Rufeng T., Dongsheng Z., Rongwang L., Xiaoyu P., Honglin F., Yuqiang L. (2020) Application of array detection technology in laser ranging, *Infrared Laser Eng.* **49**, 10, 20200006.
- 29 Degnan J.J. (2019) Possible pathways to producing rapid millimeter accuracy normal points, in: *2019 ILRS technical workshop*, Stuttgart, Germany, pp. 15.
- 30 Lebrun F., Léna P., Mignard F., Mugnier L., Pelat D., Rouan D. (2008) *L'Observation En Astrophysique*, EDP Sciences. pp. 83–95.